Manipulating Overflow Separation Directions by Wettability Boundary Positions

Zhichao Dong,[†,§] Lei Wu,[†,§] Ning Li,[§,‡] Jie Ma,[*,‡] and Lei Jiang[*,†]

[†]Beijing National Laboratory for Molecular Sciences (BNLMS), Key Laboratory of Organic Solids, Institute of Chemistry and [‡]Laboratory of Bioinspired Smart Interface Sciences (LBSIS), Technical Institute of Physics and Chemistry, Chinese Academy of Sciences (ICCAS), Beijing 100190, P. R. China and [§]University of Chinese Academy of Sciences (UCAS), Beijing 100049, P. R. China

ABSTRACT Facile strategies to realize controllable overflow separation are urgently needed for advances in liquid-directional transportation systems and liquid delivery devices. Here, we present a wettability boundary based destabilization mechanism for direct separation of liquid flow from the solid edge at the (super)hydrophilic–superhydrophobic dividing line. Macroscale fluid dynamics is precisely controlled by modifying micro- and nanoscale surface structures and chemical compositions. Coupling surface wettability boundaries with flow inertia, flow separation angles are finely adjusted. These findings not only provide physicochemical insight into the understanding of the mechanisms on the dynamics of fluid at solid edges, but also promote the development of nanoscience in hydrodynamic applications.

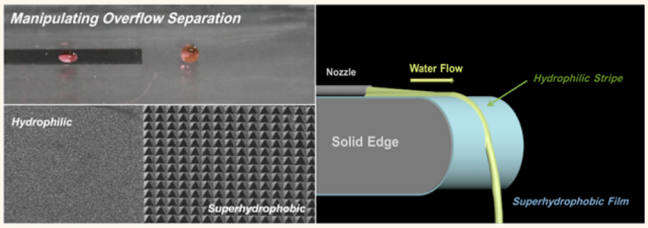

KEYWORDS: fluoride modification · dopamine modification · superwettability · overflow · flow separation

Manipulating overflow separation at solid edges is greatly needed for both fundamental research and technological applications in understanding flow dynamics at the liquid–solid interface. Controllable overflow separation means separating liquid flows at a predetermined position and ejecting flows in an intended direction. Although the ejecting direction of liquid flow can be turned by adjusting the position of nozzle opening, liquid leakage and splash always occur at the nozzle edge,[1−4] which reduces the liquid transfer efficiency and affects the directional manipulation. Recent research in interfacial science has shown that solid surfaces can be designed with special wetting properties to separate water drops or low speed fluids from a solid surface.[5−8] In particular, progress has been made for both filament breakup on flat surfaces as well as liquid separations at sharp edges. Furthermore, the recent new development of patterned superhydrophobic surfaces has shown the possibility to drive a liquid flow on the patterned surfaces.[9−13] Examples include drop emission by wetting properties in driven liquid filaments,[14] droplet ejection through micronanostructured superhydrophobic nozzles,[15,16] and stopping water dribbling by nanostructured superhydrophobic edges.[17−20] Despite these advancements, it is still challenging to manipulate the position of flow separation and dictate the direction of the ejecting flow in an open system.

Here, we present a novel method for manipulating overflow separation direction in an open system with wettability boundary positions. The surface is composed of a nanostructured hydrophilic or a superhydrophilic stripe on a round, micronanostructured superhydrophobic solid edge with a (super)hydrophilic–superhydrophobic dividing line (HSDL) in between. We found that when the position of the HSDL was fixed on the round solid edge, liquid overflowed along the nanostructured hydrophilic stripe but separated from the solid edge upon encountering the micronanostructured superhydrophobic surface. A new mechanism of instability induced by the competition between capillarity and inertia, which leads to controllable overflow separation, is demonstrated. In addition, overflow

* Address correspondence to majie@iccas.ac.cn, jianglei@iccas.ac.cn.

Received for review April 29, 2015 and accepted June 7, 2015.

Published online June 07, 2015
10.1021/acsnano.5b02580

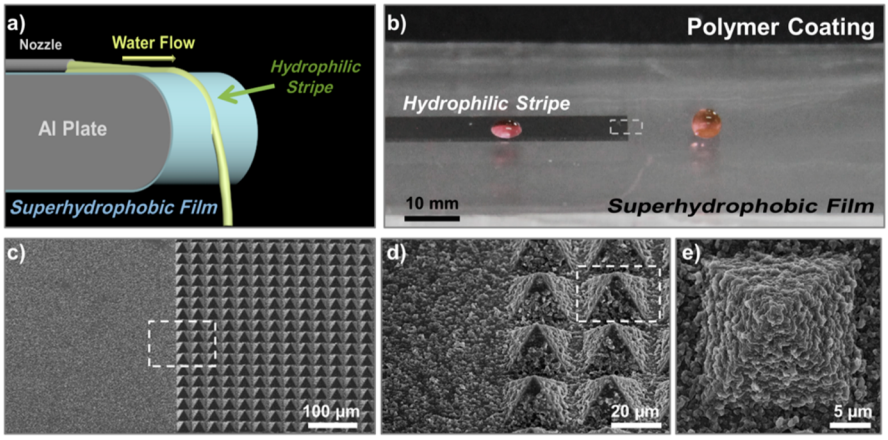

Figure 1. Experimental setup and surface morphology. (a) Scheme of experimental setup. A nozzle was mounted on the top surface of an aluminum plate. The plate's round margin was coated by a superhydrophobic polyethylene terephthalate film with a (super)hydrophilic stripe. As water exited the nozzle, it traveled along the (super)hydrophilic stripe until encountering the HSDL. (b) A 10 μL droplet of colored water kept a sphere shape on the superhydrophobic surface, while it spread on the hydrophilic stripe. (c–e) Scanning electron micrographs of the morphology differences along the HSDL. On the nanostructurd hydrophilic stripe, nanoroughness can stabilize the liquid flow firmly on the stripe. On the micronanostructured side, the air trapped between the microstructures can suspend the liquid, and nanoroughness on the microstructures could further decrease the liquid–solid contact and hence increase the liquid repellency.

separation angles were finely adjusted through the cooperative regulation of surface wettability boundaries and flow inertia. Furthermore, overflow separation
angle can be controlled from −180° counterclockwise to 180° clockwise by simply adjusting the wettability boundaries on a double-curved surface. This facile strategy is a promising candidate for the manipulation of overflow separation directions in firefighting, irrigation, drinking water systems, and other applications, which is of great significance for the development of directional liquid transportation systems.

RESULTS AND DISCUSSION

Figure 1, panel a shows the schematic diagram of the experimental setup. It is composed of a nozzle mounted on the top of an aluminum plate that had a round solid edge with a radius of curvature R of 10.0 mm. Polymer films were coated on the plate's solid edge to modify surface with wettability boundaries. The fluid used in our experiment was dyed with rhodamine 6G at a concentration of 10^{-6} g/mL. At such a low concentration, the dye molecules show little influence on the surface tension of the fluid (Figure S1, Supporting Information). Overflow separation behaviors were captured in a dark room and recorded by a digital camera with illumination from an ultraviolet lamp of 365 nm. Since longer exposure time can demonstrate the stability of flow behaviors, the exposure time is set as 10.0 s. The flow velocity was manipulated by a gear pump to achieve velocities between 0.5 and 4.0 m/s,[21] a typical flow speed range for water delivery systems such as irrigation and pipeline transportation.[22] This velocity range is in a high Reynolds number, quantifying the role of inertia versus viscosity, with the order of 10^3, and a low Weber number, expressing the impact of capillary effect versus flow inertia, with the magnitude of 10. This indicates that the viscous effect can be neglected, whereas the roles of capillary effect and surface wettability are dominant.

To separate liquid flows from the solid edge at a predetermined position, the surface wetting properties of the solid edge must satisfy two criteria: (1) successful liquid adhesion on one part of the surface and (2) low liquid–solid adhesion on the remaining part. Generally, when the surface energy of a specific surface is above 890 mJ/m^2,[23,24] the surface behaves hydrophilic and is easily wetted by water with high liquid adhesiveness. For this surface, once water overflowed along the hydrophilic or superhydrophilic curved edge (Figure S2a,b, Supporting Information), it flowed back along the bottom surface. Therefore, the first requirement can be satisfied by using a (super)hydrophilic stripe with high liquid adhesion.

For the second criterion, the surface must have a water-resistant region with low water adhesion. Solid surfaces can be made more water repellent by changing either the surface chemical composition to have low surface energies or by roughing the surface morphologies to trap air.[25] Fluorination of a smooth surface reduced the surface energy, but only moderate hydrophobicity was achieved. Figure S2c of the Supporting Information showed that overflow still existed on the smooth hydrophobic edge; thus, fluorination alone was insufficient. In contrast, superhydrophobic solid edge showed little influence on the flow dynamics of the inertial flow (Figure S2d, Supporting Information). Therefore, a structural approach for repelling water should be used to roughen the fluorinated surface with both micro- and nanostructured morphologies.

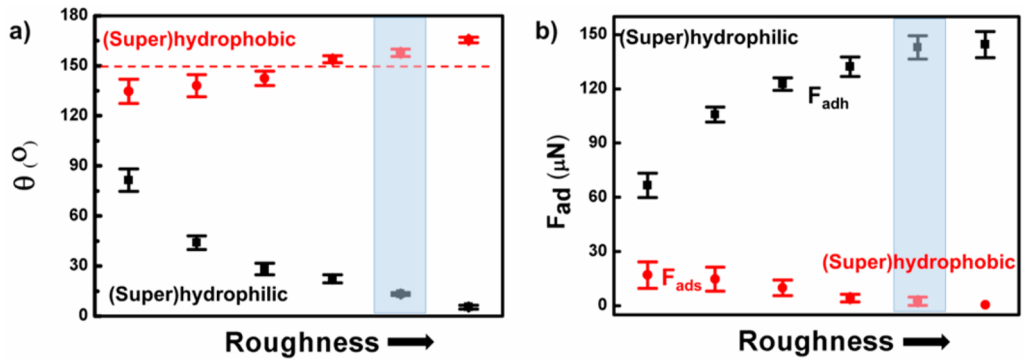

Figure 2. Surface wetting properties. (a) Contact angles θ and (b) water adhesive forces F_{ad} as a function of surface roughness. Wetting difference increased with the increase of surface roughness. Blue stripes indicate the wetting properties of the polymer coating used in Figure 1.

The air trapped between the microstructures can suspend the flowing liquid, supporting a composite interface proposed by Cassie.[26] Nanoroughness on the microstructures could further decrease the liquid–solid contact and hence increase the liquid repellency.[27−29] A coating surface with hydrophilic stripe on the micronanostructured superhydrophobic surface was thus preferred.

On the basis of the analyses above, a superhydrophobic polyethylene terephthalate (PET) coating with a 50.0 mm long and 5.0 mm wide hydrophilic stripe was prepared (Figure 1b). This PET coating was achieved by replicating the morphology of etched Si templates and selective dopamine/fluoride modification (see Experimental Section for details). Si templates were fabricated with standard photolithography, anisotropic wet etching, and metal-assisted chemical etching.[6,30] PET films were used to replicate the surface morphology of Si templates, which were then dipped into a dopamine solution and finally fluorinated in a vacuum oven with a photoresist mask (Figure S3, Supporting Information, scheme of the detailed fabrication process).[31−33] After the photoresist was stripped, specific regions of the (super)hydrophilic stripe and superhydrophobic surface were achieved with a HSDL in-between, as shown in Figure 1, panels b–e. X-ray photoelectron spectroscopy (XPS) in Figure S4 of the Supporting Information shows the surface chemical composition of the as-prepared patterned PET surface at the superhydrophobic side, which demonstrates a successful chemical selective modification that has been performed. The (super)hydrophilic–superhydrophobic patterned PET films were finally coated on the Al plate's solid edge to modify the surface with wettability boundaries.

Surface wetting properties were characterized by static contact angle θ and water adhesive force F_{ad} on the (super)hydrophilic stripe (red scatters) and superhydrophobic (black scatters) surface (Figure 2). In control experiment, a series of coating materials was fabricated and coated on the Al plate to investigate the wettability boundaries influenced overflow separation behavior. By adjusting the surface morphology of etched Si templates and selective surface chemical modification of polymer coatings, the wetting difference between the (super)hydrophilic and (super)hydrophobic regions increased with the increase of surface roughness (Figure S5a–f, Supporting Information). Blue stripes in Figure 2 indicate the wetting properties of the polymer coating in Figure 1, panels b–e, which have a θ of 5.4 ± 1.1° and a high water adhesive force F_{adh} of 132.3 ± 6.2 μN on the poly dopamine stripe, and a θ of 165.2 ± 1.7° and an ultralow water adhesive force F_{ads} of 4.3 ± 2.1 μN on the superhydrophobic surface.

Figure 3 demonstrates the manipulation of overflow separation position at solid edges with wettability boundaries. A superhydrophobic PET film with eight hydrophilic stripes, schemed in Figure 3, panel a, was coated on the plate. The deflection angles α, the flare angles between the top surface of the plate and the tangential line of the solid edge at the HSDL, were 0°, 30°, 60°, 90°, 120°, 150°, and 180°, respectively (Figure 3c–i). At a linear flow velocity of 2.0 m/s, as a paradigm, fluid overflowed along the hydrophilic stripes and separated from the solid edge at the HSDL. This facile strategy, which combines different wettabilities on the solid edge, enables precise control of overflow separation behaviors by simply adjusting the position of the HSDL.

Determination of the required hydrophilicity/hydrophobicity on both sides of the HSDL for controllable overflow separation is useful for material designs and practical applications. Theoretical analyses and experiments were both performed to make a full understanding of the wettability boundaries manipulated overflow separation. At the hydrophilic side, to stabilize the liquid flow firmly on the solid edge without separation, F_{ad} should not be less than the centripetal force that operates on the fluid (Figure 3b).[6,17] Wetting thermodynamics analysis revealed that water adhesive force, $F_{ad} \approx \gamma(1 + \cos\theta_a)S/e$, is dependent on advancing contact angle θ_a vertical to the moving direction and liquid surface tension γ.

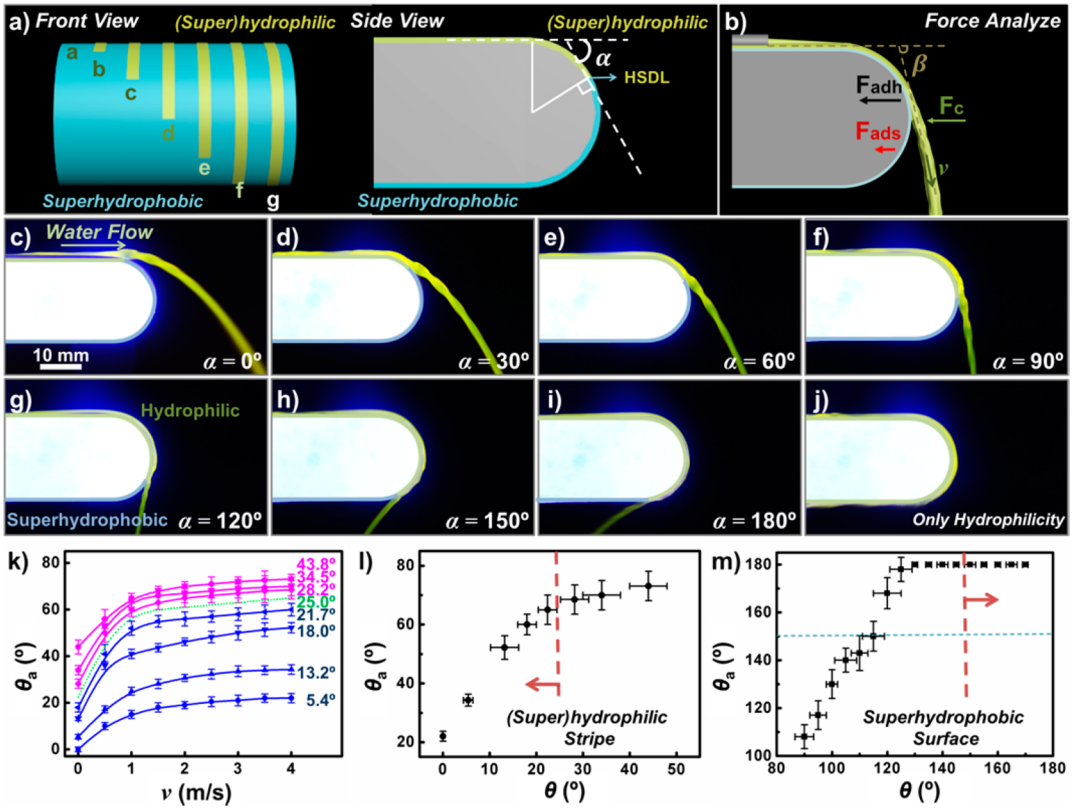

Figure 3. Controlling overflow separation positions. (a) Schematic diagram of HSDL positions set at the top surface, one-twelfth, one-sixth, one-fourth, one-third, five-twelfths, and one-half of the length of the round edge with deflection angles α ranging from 0−180°. (b) Diagram of the forces acting on the flow. Before encountering the HSDL, liquid flow clings to the hydrophilic stripe. Upon reaching the HSDL, flow separates from the solid edge with a separation angle of β. (c−i) Optical images of overflow separation behaviors at the round margin controlled by the position of the HSDL. (j) Flow behavior on a soley hydrophilic coating. The flow velocities are all 2.0 m/s for panels c−j. (k) Advancing contact angles θ_a in relation with flow velocities *v*. Scatters in panel k indicate the experimental data, and line indicates the theoretical value. Green dashed line indicates the hydrophilic surfaces with threshold advancing contact angles at varing flow velocities. Blue and red values indicate the static contact angle. (l, m) The relationship between advancing contact angles and static contact angles of the (l) (super)hydrophilic surface and (m) superhydrophobic surface with flow velocity at the maximum velocity of 4 m/s, respectively.

Since θ_a increases with flow velocity *v*, as derived by G. Friz,[34] F_{ad} is *v*-related and decreases as *v* increases. In addition, the centripetal force acting on the fluid is given by

$$F_c = \frac{\rho e S v^2}{R} \quad (1)$$

where ρ is the mass density of water, *e* is the average thickness of the liquid layer as it travels on the curved surface, and *S* is the wetted unit area.[35] F_c increases proportionally to the square of flow velocity. Thus, F_{ad} is at its minimum value when F_c operating on the fluid is at its maximum, where a threshold advancing contact angle θ_t exists at which F_c equals F_{ad}:

$$\theta_t = \cos^{-1}\left(\frac{\rho e^2 v^2}{\gamma R} - 1\right) \quad (2)$$

Therefore, only those hydrophilic coatings with θ_a smaller than θ_t can be selected to cover the curved edge.

To determine which hydrophilic surface had the upper limit static contact angle θ, a threshold value, and identified the best material for the (super)hydrophilic pattern, experiments were performed to illustrate the relationship between θ and θ_a at varied flow velocities (Figure 3k,l). As θ increased from 0° to 43.8 ± 2.7°, overflow separation (4 m/s, the maximum flow velocity) was observed at 25.6 ± 1.8°, which corresponds to θ = 25.0° (Figure 3k, green dash line), the angle determined from eq 2. Therefore, a (super)hydrophilic surface with a static contact angle <25.0° (the upper limit θ) can be used as the (super)hydrophilic pattern (Figure 3l).

At the hydrophobic side, clinging flow is theoretically predicted to separate from the solid edge if the maximum F_{ad} is less than the minimum F_c.[3,5,14] The theoretical θ_t is 124° by calculation, which is much less than the experimental minimum contact angle of 155° required for a superhydrophobic surface. Experimentally, for the surface with a θ of 124°, the overflow separation behavior indeed occurs at the HSDL when

the flow speed is less than 2.5 m/s; whereas at a flow velocity of above 3.5 m/s, overflow separation occurs after the HSDL (Figure S4, Supporting Information). This deviating flow behavior can be explained by the Coanda effect,[17] which was not considered in the above simplified model. Although F_{ad} reduced with the increasing of θ_a, an air pressure drop, which is induced by the flow itself, exists at higher flow velocities and forces the inertial flow to cling on the solid surface. To effectively separate the fluid at the HSDL, a Cassie state superhydrophobic surface with a θ greater than 155° and a F_{ad} less than 5 μN is needed and used in this experiment (Figure 3m).

In the presented surface of Figure 3, panels c−i, the wetting phase on either side of the HSDL is different: the hydrophilic side is wetted by water, while the superhydrophobic side is wetted by air.[29] In addition, at the superhydrophobic side, microstructured pyramids can act as air passages to balance the pressure drop induced by the Coanda effect, and nanostructures can destabilize the triple contact line of clinging flow.[36,37] Thus, the energy barrier induced by the air entrapment of the superhydrophobic surface can precisely force water to separate from the round solid edge at the HSDL.

We found that the overflow separation angle β can be finely adjusted by the flow velocity, though the β is not always along the tangential line of the solid edge at the HSDL (Figure 4). The difference between β and α was reduced with the increase of flow inertia, which can be clearly observed by the distances between green and red dots in Figure 4, panels a_2−d_2. This trend also occurred with other HSDL positions, as shown in Figure 4, panel g. Thus, by regulating fluid inertia and wettability boundaries cooperatively, the flow can be separated from surface in almost any determined direction.

As shown in Figure 4, panels a−d, on both sides of the HSDL, liquid flow showed different flow shapes. Above the HSDL, liquid kept an arch-shaped cross-section, while below the HSDL, separated liquid tended to form a fluid chain, a succession of mutually orthogonal links, rather than a uniform path with a disc-shaped cross-section (Figure 4a_3−d_3). This phenomenon is an everyday occurrence when pouring juice from a lipped jug and rivulets flowing off a leaf or sharp edge.[38] The velocity of the inner flow, in contact with the hydrophilic stripe, slows due to the restriction force, while the velocity of the outer flow, in contact with the air−superhydrophobic-surface interface, is not influenced.[38] Thus, the separating flow could not flow at an equal speed across the HSDL.

Flow velocity influences the shape of fluid chain, which can further affect the overflow separation direction. A thorough analysis of the relationship between (β − α) and v was performed. The collision of high

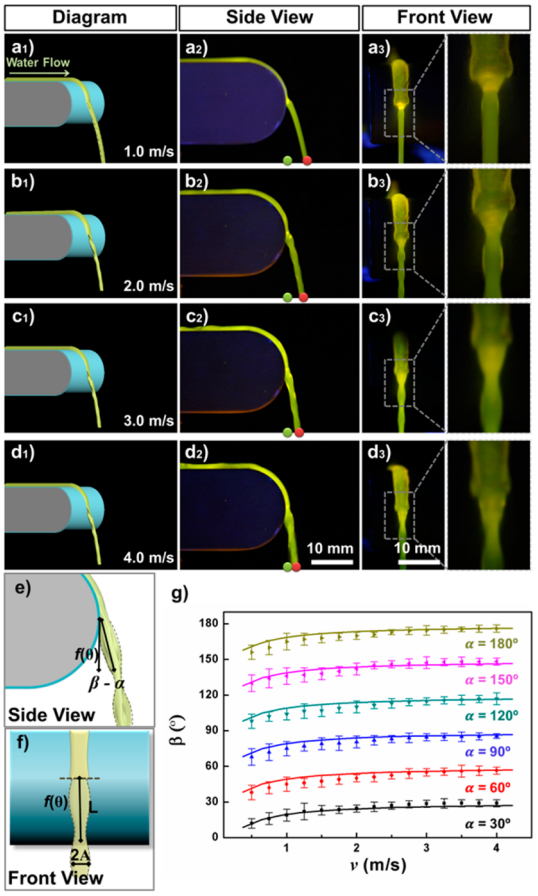

Figure 4. Manipulating overflow separation angles. (a_1−d_1) Schematic images, (a_2−d_2) side view, and (a_3−d_3) front view optical images of velocity dependent overflow separation behaviors. (e) Side and (f) front view diagrams showing the double-sine-curve flow chain profile. Fluid chain exists when liquid separates from the solid edge. Separation position, α, affects the overflow separation angle, β, and flow velocity precisely regulated β. (g) The relationship between β and α with the variation of flow velocities. The difference between β and α slightly decreases with the increase of flow velocities, and the separation angle β was manipulated from 3° to 180° by regulating the flow velocity and the position of the HSDL.

speed outer flows at the HSDL, which is similar to the obliquely colliding jets,[38−40] generates a fluid sheet perpendicular to the solid surface (Figure 4e,f). Within the sheet, fluid shoots radially away from the point of the HSDL at roughly uniform speeds. The sheet thins with 1/r, where r is the radial distance of the point of separation, until reaching the sheet's edge. A double sine curve-like separated flow is thus produced, and the profile of a sine curve near the solid edge is regarded as $f(\theta) = A \sin \theta$, where A is the amplitude of the sine curve, and θ is the contact angle. Since the superhydrophobic surface can prevent the liquid from wetting the solid edge and shows no influence on the flow dynamics,[6] the separating flow is along the direction of the slope of the oscillation chain at the HSDL. In addition, the slope of the fluid chain is parallel with the tangent line of the difference between the over-

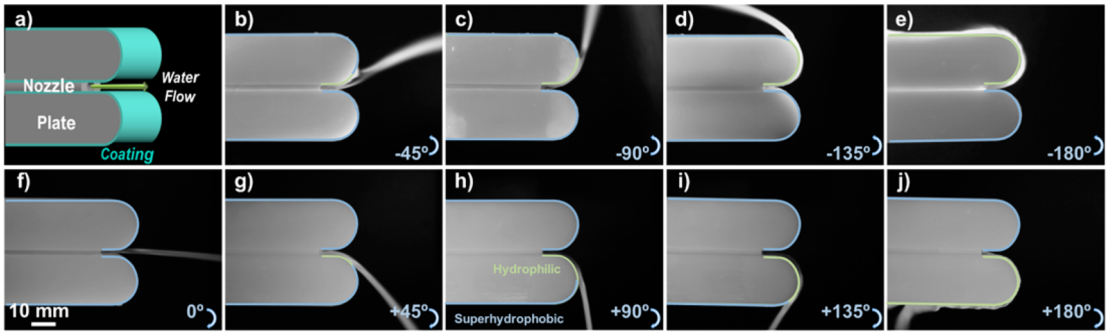

Figure 5. Overflow separation in controllable directions. (a) Schematic diagram showing the experimental setup. A nozzle was mounted between two plates such that water flow could travel along both sides of the plate before encourting the round edges. (b–j) Images of the flow dynamics on the double cureved plate. (b–e) The downward curved plate had a superhydrophobic coating, while the upward curved plate was coated to have wettability boundaries, with a HSDL at (b) one-eighth, (c) one-fourth, (d) three-eighths, and (e) one-half of the circle circumference, counterclockwise. Ejecting flow separated upward from the round margin at the HSDL. (f) Both plates had superhydrophobic coatings. The flow ejected horizonally. (g–j) The upward curved plate had a superhydrophobic coating, and the downward curved plate was coated to have wettability boundaries with a HSDL at (g) one-eighth, (h) one-fourth, (i) three-eighths, and (j) one-half of the circle circumference, clockwise. Ejecting flow separated clockwise from the round margin at the HSDL.

flow separation angle β and the deflection angle α.[41] Following the mathematical derivation of the slope of $f(\theta)$, $\tan(\beta - \alpha) \approx (A/L)\pi \cos\theta_a$, where A is the amplitude of the curve, L is the wavelength of the curve, and θ_a is the advancing contact angle. In addition, the wavelength L of the oscillation chain is quantitatively related with flow velocity v, which can be expressed as $L = \pi r v(2\rho r/3\gamma)^{1/2}$, where r is the radial distance of the point of separation, v is the flow velocity, ρ is the liquid density, and γ is the surface tension.[41−43] By using the theoretical result of L, $(\beta - \alpha) \approx \tan^{-1}(k/v)$. For a predetermined liquid, k is a constant; thus, $(\beta - \alpha)$ depends on v. As v increases from 0.5 to 4.0 m/s, $(\beta - \alpha)$ changes from 0 to 30°.

In the experiment, as shown in Figure 4, panel g, with flow velocities varying from 0.5−4.0 m/s and α setting at 30°, 60°, 90°, 120°, 150°, and 180°, respectively, liquid flow was controlled to separate from the solid edge with β ranging from 3−180°, which fits the theoretical results. Moreover, the separation angle at low speed is lower than that at high speed, which can be explained more qualitatively by the competition between the act of surface superhydrophobicity and flow inertia. At low speed, the act of surface superhydrophobicity can force the fluid separating from the solid edge at the HSDL with a separation angle $(\beta - \alpha)$, while the flow inertia, at high flow speed, acts to hold its original flow direction to decrease this angle. Therefore, with the cooperation of HSDL and flow velocity, the overflow separation direction can be finely manipulated experimentally and theoretically.

A prototype of application for this wettability boundaries controlled overflow separation is demonstrated using the following setup. As shown in Figure 5, the overflow separation direction could be controlled either upward or downward with varied separation angles by simply adjusting the HSDL position. A nozzle was placed between two round plates such that water flow can travel along the surfaces on both sides (Figure 5a). Since the superhydrophilic pattern can strongly attract the flow, water overflowed the upper plate when the downward curved plate was modified with a superhydrophobic coating. When the HSDL was set at one-eighth, one-fourth, three-eighth, or one-half the circumference of the round edge counterclockwise, ejecting flow separated upward at corresponding angles (Figure 5b–e). Similarly, when the HSDL was set at the downward round edge at various clockwise positions, ejecting flow separated downward at corresponding angles (Figure 5g–i). When both plates were modified to be superhydrophobic, the liquid ejected horizontally (Figure 5f). Therefore, if the opening of a tube is selectively modified with wettability boundaries on one part and superhydrophobicity on the other part, water flow can be controlled to separate from the solid edge at predetermined positions and directions without the use of changing the direction of nozzle opening.

CONCLUSION

In conclusion, we constructed a series of surfaces with wettability boundaries to control overflow separation behaviors at solid edges. Macroscale fluid dynamics is manipulated by the micro- and nanoscale surface structures and chemical compositions. Overflow separation was triggered at the predetermined position of the (super)hydrophilic−superhydrophobic dividing line, and overflow separation angle was manipulated through cooperatively regulating the position of wettability boundaries and the flow inertia. This fundamental research will guide rational fabrication of

coating materials at solid edges to control overflow separation behaviors and accelerate the development of materials with wettability boundaries to manipulate the flow hydrodynamics at solid edges.

EXPERIMENTAL SECTION

Materials. PET films with a thickness of 1.0 mm were obtained from 3 M Co. Ltd. Positive resist PR1−2000A and RD-6 developer were purchased from Futurrex, Inc. 1H,1H,2H,2H-Perfluorodecyltrimethoxysilane (PFOS) and dopamine were purchased from Sigma-Aldrich. The ⟨100⟩-oriented silicon wafer with 500 nm SiO_2 covered on the top layer was purchased from Institute of Semiconductors, Tianjin, China.

Sample Preparation. PET coatings with micro/nanostructures were achieved by replicating the morphology of corresponding etched Si templates. PET was used as replicas. The negative micro/nanostructured Si template was obtained from standard photolithography, anisotropic wet etching, and metal-assisted chemical etching.

Fabrication of Si Template and PET Film. According to our previous method,[6] a thin layer of positive resist was spray-coated onto a SiO_2 covered silicon wafer at a rotational speed of 3000 rpm, which was followed by a UV exposure process. The photomask had a 50.0 mm long and 5.0 mm wide light blocking stripe and four positioning patterns. Then, the UV exposed Si wafer was immerged into a buffered oxide etching solution to remove the unprotected SiO_2 layer. Subsequently, the as-prepared substrate was put into a KOH solution for orientational erosion. After it was rinsed with ultrapure water and dried with N_2 flow, the microstructured Si wafer composed of inverse pyramidal arrays was acquired. To obtain the nanostructures, metal-assisted chemical etching was used to roughen the as-prepared microstructured Si wafer. Au film was vacuum evaporated onto the inverse pyramidal arrays and then annealed into dot-arrays at 1173 K with temperature increasing from 293 K to 1173 K at the speed of 200 K/h, and holding at 1173 K for 4 h before cooling in a muffle furnace. These arrayed Au dots acted as microscopic catalysts in drilling nanoholes into the microstructured Si substrate. After etching in a HF solution, micro-nanostructured Si template was thus finally achieved. A 0.5 mm thick PET film was used to copy the morphology of Si template at 520 K.

Polydopamine Coating and Selective Fluorination. A sample of 0.1 g of dopamine was added to 10 mL of Tris-HCl (10 mM) at pH = 8.5 with stirring at 300 rpm for 30 min. Oxidation changes the color of solution from colorless to dark brown. Hydrophilic PET films were dipped into the as-prepared solution twice at the advancing speed of 0.80 mm/s, and retraction speed of 0.80 mm/s, the holding time of which is 600 s. A thin layer of polydopamine was covered on the hydrophilic PET surface. A thin layer of positive resist was then spray-coated onto the polydopamine-coated PET film at a rotational speed of 3000 rpm, which was followed by a UV exposure process. During the exposure process, a photomask with only a 50.0 mm long and 5.0 mm wide light blocking stripe was used. Caution: the photomask must be focused to local the position with the help of positioning patterns. After UV exposure, the as-prepared PET film was fluorinated in a vacuum desiccator with 10 μL of PFOS at 353 K for 3 h. The fluorinated PET film was rinsed with acetone, ethanol, water, and dried by N_2 gas. The (super)hydrophilic−superhydrophobic patterned surface was finally achieved.

Instruments and Characterizations. Scanning electron microscope (SEM) images were captured by a field-emission scanning electron microscope at 10 kV (JEOL-7500F, Japan). Contact angles were measured on an OCA 20 machine (Germany) and were obtained by measuring more than five different positions on the coating surfaces. The adhesive force was measured by removing a 10 μL droplet from the solid surfaces by using a high-sensitivity microelectromechanical balance system with a resolution of 10 μg (DataPhysics DCAT 11, Germany). Optical images were captured in a dark room by a Nikon D90 digital camera with illumination from an ultraviolet lamp of 365 nm.

Conflict of Interest: The authors declare no competing financial interest.

Acknowledgment. We acknowledge project funding provided by the National Research Fund for Fundamental Key Projects (2012CB934101, 2012CB933202, 2013CB933000), the National Natural Science Foundation (21121001, 91127025), and the Key Research Program of the Chinese Academy of Sciences (KJZD-EW-M01).

Supporting Information Available: Flow behaviors at solid edges with superhydrophilicity, hydrophilicity, hydrophobicity, and superhydrophobicity; fabrication steps for (super)hydrophilic−superhydrophobic surfaces, the relationship between surface morphologies, and wetting properties. The Supporting Information is available free of charge on the ACS Publications website at DOI: 10.1021/acsnano.5b02580.

REFERENCES AND NOTES

1. Reiner, M. The Teapot Effect. *Phys. Today* **1956**, *9*, 16–20.
2. Walker, J. The Troublesome Teapot Effect, or Why a Poured Liquid Clings to the Container. *Sci. Am.* **1984**, *251*, 144–145.
3. Clanet, C. Waterbells and Liquid Sheets. *Annu. Rev. Fluid Mech.* **2007**, *39*, 469–496.
4. Scardovelli, R.; Zaleski, S. Direct Numerical Simulation of Free-Surface and Interfacial Flow. *Annu. Rev. Fluid Mech.* **1999**, *31*, 567–603.
5. Duez, C.; Ybert, C.; Clanet, C.; Bocquet, L. Making a Splash with Water Repellency. *Nat. Phys.* **2007**, *3*, 180–183.
6. Dong, Z.; Wu, L.; Wang, J.; Ma, J.; Jiang, L. Superwettability Controlled Overflow. *Adv. Mater.* **2015**, *27*, 1745–1750.
7. Xu, J. H.; Luo, G. S.; Li, S. W.; Chen, G. G. Shear Force Induced Monodisperse Droplet Formation in a Microfluidic Device by Controlling Wetting Properties. *Lab Chip* **2006**, *6*, 131–136.
8. Bird, J. C.; Dhiman, R.; Kwon, H. M.; Varanasi, K. K. Reducing the Contact Time of a Bouncing Drop. *Nature* **2013**, *503*, 385–388.
9. Mumm, F.; van Helvoort, A. T.; Sikorski, P. Easy Route to Superhydrophobic Copper-Based Wire-Guided Droplet Microfluidic Systems. *ACS Nano* **2009**, *3*, 2647–2652.
10. Oliveira, N. M.; Neto, A. I.; Song, W. L.; Mano, J. F. Two-Dimensional Open Microfluidic Devices by Tuning the Wettability on Patterned Superhydrophobic Polymeric Surface. *Appl. Phys. Express* **2010**, *3*, 085205–085205.
11. Lai, Y. K.; Pan, F.; Xu, C.; Fuchs, H.; Chi, L. F. *In Situ* Surface-Modification-Induced Superhydrophobic Patterns with Reversible Wettability and Adhesion. *Adv. Mater.* **2013**, *25*, 1682–1686.
12. Sousa, M. P.; Mano, J. F. Patterned Superhydrophobic Paper for Microfluidic Devices Obtained by Writing and Printing. *Cellulose* **2013**, *20*, 2185–2190.
13. Lai, Y.; Lin, L.; Pan, F.; Huang, J.; Song, R.; Huang, Y.; Lin, C.; Fuchs, H.; Chi, L. Bioinspired Patterning with Extreme Wettability Contrast on TiO_2 Nanotube Array Surface: A Versatile Platform for Biomedical Applications. *Small* **2013**, *9*, 2945–2953.
14. Ledesma-Aguilar, R.; Nistal, R.; Hernandez-Machado, A.; Pagonabarraga, I. Controlled Drop Emission by Wetting Properties in Driven Liquid Filaments. *Nat. Mater.* **2011**, *10*, 367–371.
15. Dong, Z. C.; Ma, J.; Jiang, L. Manipulating and Dispensing Micro/Nanoliter Droplets by Superhydrophobic Needle Nozzles. *ACS Nano* **2013**, *7*, 10371–10379.
16. Byun, D.; Lee, Y.; Tran, S. B. Q.; Nugyen, V. D.; Kim, S.; Park, B.; Lee, S.; Inamdar, N.; Bau, H. H. Electrospray on

Superhydrophobic Nozzles Treated with Argon and Oxygen Plasma. *Appl. Phys. Lett.* **2008**, *92*, 093507–093507.
17. Duez, C.; Ybert, C.; Clanet, C.; Bocquet, L. Wetting Controls Separation of Inertial Flows from Solid Surfaces. *Phys. Rev. Lett.* **2010**, *104*, 084503–084503.
18. Mertaniemi, H.; Jokinen, V.; Sainiemi, L.; Franssila, S.; Marmur, A.; Ikkala, O.; Ras, R. H. Superhydrophobic Tracks for Low-Friction, Guided Transport of Water Droplets. *Adv. Mater.* **2011**, *23*, 2911–2914.
19. Zhang, J.; Gao, X.; Jiang, L. Application of Superhydrophobic Edge Effects in Solving the Liquid Outflow Phenomena. *Langmuir* **2007**, *23*, 3230–3235.
20. Sheng, X.; Zhang, J.; Jiang, L. Application of the Restricting Flow of Solid Edges in Fabricating Superhydrophobic Surfaces. *Langmuir* **2009**, *25*, 9903–9907.
21. Gennes, P. G.; Brochard-Wyart, F.; Quere, D. *Capillarity and Wetting Phenomena: Drops, Bubbles, Pearls, Waves*; Springer Science & Business Media: New York, 2004.
22. Liebe, R. *Flow Phenomena in Nature: Inspiration, Learning, and Application*; WIT Press: Southampton, UK, 2007; Vol. 2.
23. Kinloch, A. J. *Adhesion and Adhesives: Science and Technology*; Springer Science & Business Media: New York, 1987.
24. Holländer, A. On the Selection of Test Liquids for the Evaluation of Acid−Base Properties of Solid Surfaces by Contact Angle Goniometry. *J. Colloid Interface Sci.* **1995**, *169*, 493–496.
25. Feng, L.; Li, S.; Li, Y.; Li, H.; Zhang, L.; Zhai, J.; Song, Y.; Liu, B.; Jiang, L.; Zhu, D. Superhydrophobic Surfaces: From Natural to Artificial. *Adv. Mater.* **2002**, *14*, 1857–1860.
26. Cassie, A. B. D.; Baxter, S. Wettability of Porous Surfaces. *Trans. Faraday Soc.* **1944**, *40*, 0546–0550.
27. Gao, X.; Jiang, L. Water-Repellent Legs of Water Striders. *Nature* **2004**, *432*, 36–36.
28. Ball, P. Material Witness: Natural Waterproofing. *Nat. Mater.* **2009**, *8*, 250–250.
29. Snoeijer, J. H.; Andreotti, B. Moving Contact Lines: Scales, Regimes, and Dynamical Transitions. *Annu. Rev. Fluid Mech.* **2013**, *45*, 269–292.
30. Kang, S. M.; You, I.; Cho, W. K.; Shon, H. K.; Lee, T. G.; Choi, I. S.; Karp, J. M.; Lee, H. One-Step Modification of Superhydrophobic Surfaces by a Mussel-Inspired Polymer Coating. *Angew. Chem., Int. Ed.* **2010**, *49*, 9401–9404.
31. Lee, H.; Dellatore, S. M.; Miller, W. M.; Messersmith, P. B. Mussel-Inspired Surface Chemistry for Multifunctional Coatings. *Science* **2007**, *318*, 426–430.
32. Ueda, E.; Levkin, P. A. Emerging Applications of Superhydrophilic−Superhydrophobic Micropatterns. *Adv. Mater.* **2013**, *25*, 1234–1247.
33. Lepoittevin, B.; Bedel, S.; Dragoé, D.; Bruzaud, J.; Barthés-Labrousse, M.-G.; Mazerat, S.; Herry, J.-M.; Bellon-Fontaine, M.-N.; Roger, P. Antibacterial Surfaces Obtained through Dopamine and Fluorination Functionalizations. *Prog. Org. Coat.* **2015**, *82*, 17–25.
34. Friz, G. On the Dynamic Contact Angle in the Case of Complete Wetting. *Z. Angew. Phys.* **1965**, *19*, 374–378.
35. Drazin, P. G.; Reid, W. H. *Hydrodynamic Stability*; Cambridge University Press: Cambridge, UK, 2004.
36. Benkreira, H.; Khan, M. I. Air Entrainment in Dip Coating under Reduced Air Pressures. *Chem. Eng. Sci.* **2008**, *63*, 448–459.
37. Tsai, P. C.; van der Veen, R. C. A.; van de Raa, M.; Lohse, D. How Micropatterns and Air Pressure Affect Splashing on Surfaces. *Langmuir* **2010**, *26*, 16090–16095.
38. Bush, J. W. M.; Hasha, A. E. On the Collision of Laminar Jets: Fluid Chains and Fishbones. *J. Fluid Mech.* **2004**, *511*, 285–310.
39. Kibar, A.; Karabay, H.; Yigit, K. S.; Ucar, I. O.; Erbil, H. Y. Experimental Investigation of Inclined Liquid Water Jet Flow onto Vertically Located Superhydrophobic Surfaces. *Exp. Fluids* **2010**, *49*, 1135–1145.
40. Krechetnikov, R. Stability of Liquid Sheet Edges. *Phys. Fluids* **2010**, *22*, 092101.
41. Rayleigh, L. On the Capillary Phenomena of Jets. *Proc. R. Soc. London* **1879**, *29*, 71–97.
42. Epikhin, V.; Kulago, A.; Shkadov, V. Y. Motion of a Non-isothermal Jet in a Field of Centrifugal Forces. *Fluid Dyn.* **1980**, *15*, 656–663.
43. Celestini, F.; Kofman, R.; Noblin, X.; Pellegrin, M. Water Jet Rebounds on Hydrophobic Surfaces: A First Step to Jet Microfluidics. *Soft Matter* **2010**, *6*, 5872–5876.